UDC 544.032.4+ 544.015

DOI: 10.15372/CSD2019181

Electrode Material for Supercapacitors Based on Carbon/Nickel Cobaltate Nanocomposite Synthesized by the Thermal Decomposition of Cobalt and Nickel Azides

T. A. LARICHEV[1], N. M. FEDOROVA[1], G. YU. SIMENYUK[2], YU. A. ZAKHAROV[1,2], V. M. PUGACHEV[1], V. G. DODONOV[1], D. G. YAKUBIK[1]

[1]*Kemerovo State University, Kemerovo, Russia*

E-mail: timlar@kemsu.ru

[2]*Federal Research Centre of Coal and Coal Chemistry, Siberian Branch, Russian Academy of Sciences, Kemerovo, Russia*

Abstract

Structural, morphological and electrochemical properties of the electrode material for supercapacitors which consists of a porous matrix with embedded mixed cobalt-nickel oxide nanoparticles were investigated. The synthesis of the nanostructured composite was carried out by thermal decomposition of mixed nickel and cobalt azides on the surface of multi-wall carbon nanotubes. X-ray diffraction analysis and small-angle scattering were used to determine the composition and to estimate the dispersion characteristics of the obtained oxide nanoparticles. Investigation of the electrochemical properties of synthesized electrode materials by means of cyclic voltammetry showed that the growth of their electrical capacity is proportional to an increase in the content of nickel cobaltate $NiCo_2O_4$ in the composite, while the dependence for cobalt oxide Co_3O_4 is more complicated. Electrode materials based on nanostructured carbon – nickel cobaltate composite $C/NiCo_2O_4$ provide a significant increase in electrical capacity, compared to the capacity of the original carbon matrix.

Keywords: nickel cobaltate, cobalt oxide, cobalt azide, nickel azide, carbon nanotube, supercapacitor

INTRODUCTION

Supercapacitors (ionistors) are promising devices accumulating electric energy [1]. The ability of supercapacitors to accumulate energy is to a substantial extent determined by the properties of electrode materials used in these devices, so at present, we witness intense development of methods to obtain such materials combining high electric capacity with the ability to be recharged many times without deterioration of the characteristics, ecological safety and cheapness of production. One of the most popular schemes is based on the use of nanostructured composite materials composed of a porous electroconductive matrix and nanometer-sized particles of the oxides of metals with variable valence [2].

During recent years, it is increasingly frequently proposed to use the phases of a complicated composition containing mixed or doped oxides as the oxide material [3]. These phases possess advantages in the accumulation of electric charge, increased electrical conduction, *etc*. However, the fabrication of nanostructured electrode materials with complicated composition is a rather labour-intensive problem.

In the present work, we consider the possibility to obtain an electrode material with compli-

cated composition using a rather simple procedure of thermal decomposition of inorganic azides. As a rule, in the exothermal reaction of azide decomposition, nanosized metal particles are formed along with molecular nitrogen [4]. In the oxidative atmosphere (in the presence of oxygen) and at increased temperature, metal nanoparticles would be most likely transformed into the oxides of the corresponding metals. If cocrystallized azides of different metals are used as initial material, then the particles of corresponding mixed oxides may be formed as a result of thermal decomposition and oxidation. However, the question concerning the actual composition of the products of these transformations in complicated mixtures still remains open.

The goal of the present work was to study the regularities of the formation of electrode composite material formed during the thermal decomposition of the mixed cobalt–nickel azide inserted into the porous carbon matrix. The molar ratio of cobalt and nickel azides was 2 : 1, which could hypothetically provide the formation of nickel cobaltate ($NiCo_2O_4$) as the oxide phase, and this compound possesses a number of advantages for use in the electrode material [5, 6]. For comparison, we studied the regularities of the formation of composite based on cobalt (I, III) oxide obtained as a result of thermal decomposition of cobalt azide, and multilayer carbon nanotubes (MCNT) – Co_3O_4/MCNT.

EXPERIMENTAL

Reagents and materials

The matrix for obtaining nanocomposite was carbon material of MCNT type submitted by the Institute of Coal Chemistry and Chemical Materials Science of the FRC CCC SB RAS. The material was composed of multiwall nanotubes with total specific surface 250 m^2/g, outer diameter of the tubes 10–20 nm and inner diameter 6–10 nm.

The solutions of reagents were prepared using $CoCl_2 \cdot 6H_2O$, $NiCl_2 \cdot 6H_2O$ and NaN_3 of ch. d. a. (analytically pure) reagent grade. To obtain cobalt-nickel azide providing the total cobalt and nickel content in the composite 1, 5, 10 and 20 mass %, we used the mixtures of two volumes of $CoCl_2$ (0.1 M) solution and one volume of $NiCl_2$ (0.1 M) solution in the necessary amounts.

To obtain the composite material, the weighted portions of the MCNT matrix (m = 200 mg) were ground in an agate mortar and transferred into a weighing bottle. The carbon matrix was impregnated in the weighing bottle for 1 h in a mixture of the solutions of $CoCl_2$ and $NiCl_2$. After impregnation, the solution of NaN_3 was added into the bottle to obtain cobalt – nickel azide according to the exchange reaction

$$NiCo_2Cl_6 + 6NaN_3 \rightarrow NiCo_2(N_3)_6 + 6NaCl \quad (1)$$

The resulting mixture was dried in the air for 24 h, then it was transferred onto a paper filter on Buchner funnel conjugated with Bunsen flask and washed with distilled water from sodium chloride. After washing, the composite was dried on the funnel at T = 25 °C. Thermal decomposition of the composite material $C/NiCo_2(N_3)_6$ was carried out in the Tulyachka-2 drying box in two stages: 1) 60 min at 120 °C (heating rate ~2 °C/min); 2) 240 min at 270 °C in the air (heating rate ~1 °C/min).

The assumed scheme of the decomposition of mixed cobalt – nickel azide is:

$$NiCo_2(N_3)_6 \rightarrow Ni + 2Co + 9N_2 \quad (2)$$

and it is very probable that one may expect the formation of the metal phase in the form of an alloy of cobalt and nickel.

The resulting fine metal particles were oxidized at increased temperature and in the oxygen-containing atmosphere to form nickel cobaltate:

$$Ni + 2Co + 2O_2 \rightarrow NiCo_2O_4 \quad (3)$$

The data on the composition of the synthesized samples and their designations are presented in Table 1. The figures in sample designations point to the total mass content of metals introduced into the carbon material. For example, for the $NiCo_2O_4$/MCNT-1 sample, the mass content of nickel and cobalt is 1 %.

TABLE 1

Designations of samples and calculated composition of the composite material

Sample designation	Calculated mass fraction of metals in the composite, mass %
$NiCo_2O_4$/MCNT-1	1
$NiCo_2O_4$/MCNT-5	5
$NiCo_2O_4$/MCNT-10	10
$NiCo_2O_4$/MCNT-20	20
Co_3O_4/MCNT-1	1
Co_3O_4/MCNT-5	5
Co_3O_4/MCNT-10	10
Co_3O_4/MCNT-20	20

Physicochemical methods

Electron microscopic studies were carried out with a JEOL JEM 2100 transmission electron microscope (Japan).

Diffraction and X-ray fluorescence (XP) spectra were recorded with a Difrey 401 X-ray diffractometer (Russia) in monochromatic FeK_α radiation (λ = 1.9373 Å) with the embedded energy-dispersive detector Amptek (USA).

The measurements of the intensity of small-angle scattering (SAS) were carried out with the help of a KRM-1 diffractometer (Russia) in the transmission mode in the characteristic radiation of iron by means of counting the pulses in points within the range 0.002–0.35 Å^{-1}. These SAS spectra were used to calculate the size distribution of nonuniformities (particles) [7].

Electrochemical measurements were carried out with a Parstat 4000 potentiostat/galvanostat (Princeton Applied Research, USA) in a two-electrode cell with electrodes made of stainless steel and a Nafion separator. A 6 M KOH solution was used as the electrolyte.

To study the properties of the composites, an asymmetric design of the cell was chosen. A hybrid electrode material based on nanocomposites containing nickel cobaltate was used as the working electrode, while the initial MCNT matrix was used as the counter-electrode. The capacity of the cell was determined from the area limited by the curves recorded with cyclic voltammetry (CVA):

$$C_{cell} = q/Um \quad (4)$$

Here C_{cell} is the capacity of the cell, F/g; q is the charge accumulated by the cell, C; U is the potential difference, V; m is electrode mass, g.

Capacities of electrodes were determined using equation

$$C_{el} = C_{cell}C_0/(C_0 - C_{cell}) \quad (5)$$

Here C_{cell} is the capacity of the electrode cell; C_{el} is the capacity of the working electrode; C_0 is the capacity of counter-electrode.

RESULTS AND DISCUSSION

The electron microphotographs of initial carbon material MCNT are shown in Fig. 1. The difference in the inner structure of carbon fibres is evident (see Fig. 1, *b*). The walls of carbon tubes are formed by 10–15 atomic carbon layers. The nanotubes are characterized by rather broad size distribution, both in diameter and in length.

It was demonstrated at the qualitative level by means of X-ray fluorescence analysis that the amount of cobalt and nickel in the composite increases with an increase in the preassigned metal content in the sequence from $NiCo_2O_4$/MCNT-1 to $NiCo_2O_4$/MCNT-20. The intensity of the cobalt signal in the XRF spectrum in all cases is about two times as high as the intensity of the nickel signal. The quantitative determination of nickel and cobalt content in the case of their joint presence is hindered for this method by the overlap of the characteristic lines of metals and iron radiation of the tube (FeK_β is overlapping with CoK_α, while CoK_β is overlapping with NiK_α) in the XRF spectrum.

The diffraction patterns of the composite samples are shown in Fig. 2. They confirm the formation of the spinel phase, namely nickel cobaltate, in the thermal decomposition of nickel and cobalt azides. The observed diffraction maxima (reflections) 39.5, 46.6, 57.0, 76.6 and 85.0° over 2θ correspond to the spinel phase $NiCo_2O_4$ with lattice parameter 8.116(3) Å (according to the database ICDD 8.114 Å). The presence of reflection 220 near 40°, which is characteristic of spinels, and

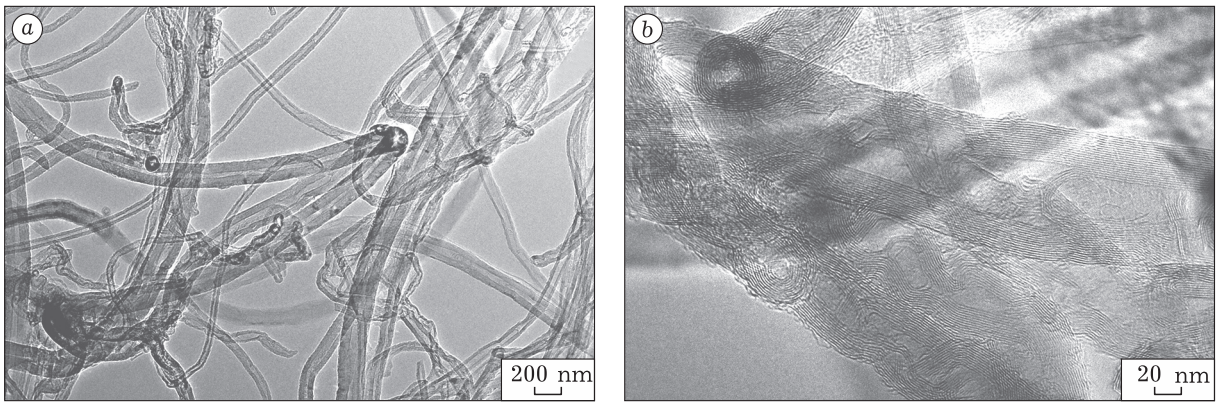

Fig. 1. Electron microphotographs of initial carbon material MCNT at different magnifications.

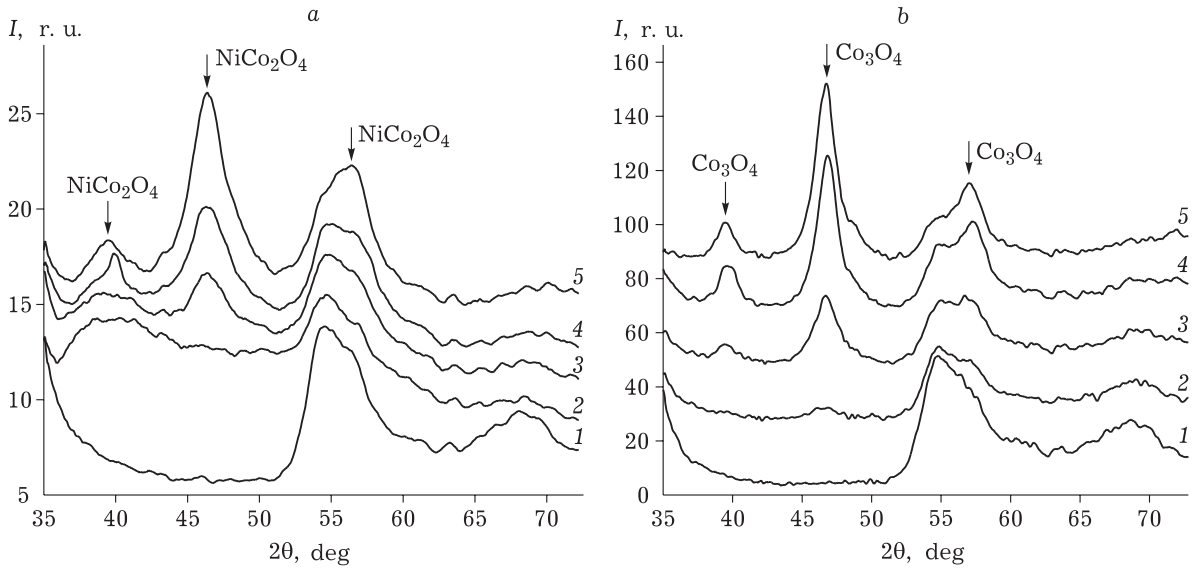

Fig. 2. Diffraction patterns of the composite materials $NiCo_2O_4$/MCNT-x (*a*) and Co_3O_4/MCNT-x (*b*). x is metal content in the samples, mass %: 0 (*1*), 1 (*2*), 5 (*3*), 10 (*4*), 20 (*5*).

the absence of one of the strong reflections of NiO 82.0° (220 the structural type of NaCl) provide evidence that metals are localized mainly in the spinel phase. With an increase in metal content in the composites, the diffraction spectrum of the matrix weakens, while a weaker shoulder of the strongest complex maximum (≈55°) from the side of larger angles is increasingly stronger overlapped with one of the lines of spinel. The size of the crystallites of the oxide phase estimated from reflection broadening (Scherrer method) is 5–10 nm.

In the case of the composite obtained through thermal decomposition of pure cobalt azide, results of X-ray phase analysis show that the final product of decomposition is cobalt (II, III) oxide. The diffraction patterns of the samples (see Fig. 2, *b*) are represented by the broad lines of the fine spinel phase Co_3O_4: 39.6, 46.8, 57.2, 77.0, 85.2° with lattice parameters 8.092(3) Å (according to database ICDD 8.084 Å). The size of crystallites determined from reflection broadening (Scherer method) is 4–5 nm. The absence of the lines of metal cobalt (56.2 and 66.0°) and a strong reflection 220 CoO (80.0°) points to the phase homogeneity of the final product of decomposition. With an increase in the assigned cobalt content in the sample, the intensities of the maxima corresponding to the Co_3O_4 phase increases.

The experimental SAS curves for nanocomposite samples with the composition $NiCo_2O_4$/MCNT are presented in Fig. 3, *a*. All curves corresponding to nanocomposites (except $NiCo_2O_4$/MCNT-1) contain an additional signal which may be due to the presence of filler in the samples of the phase (dash line shows the subtrahend MCNT function). The region of the lengths of scattering vectors where an additional signal appears (0.06–0.07 $Å^{-1}$) is obviously to the right from the basic maximum, $J(s) \cdot s^2$ for the pure matrix (0.01–0.02 $Å^{-1}$). This means qualitatively that additional scattering is mainly due to nonuniformities of smaller size.

The mass (volume) size distribution functions $D_m(d)$ calculated from scattering curves for the pure MCNT matrix and nanocomposite samples are presented in Fig. 3, *b*. The dispersed structure of the carbon matrix is characterized by clearly pronounced bimodal distribution (maxima at 5 and 17 nm). It is noteworthy that the distribution of nonuniformities in the composite is also bimodal, with the positions of maxima insignificantly shifted with respect to the maxima of the initial carbon matrix. The shift of the position of the first maximum towards smaller size is clearly seen even for general functions $D_m(d)$ (see Fig. 3, *b*). However, the differential signal looks more complicated (see Fig. 3, *c*). The position of the main maximum for the differential $D_m(d)$, as expected, does not coincide with the pure MCNT matrix and lies in the region of smaller size (4 nm). Its intensity increases regularly with an increase in the percentage of metal content. Oscillations of the right wing of the differential $D_m(d)$ are likely to be nonrandom because they are re-

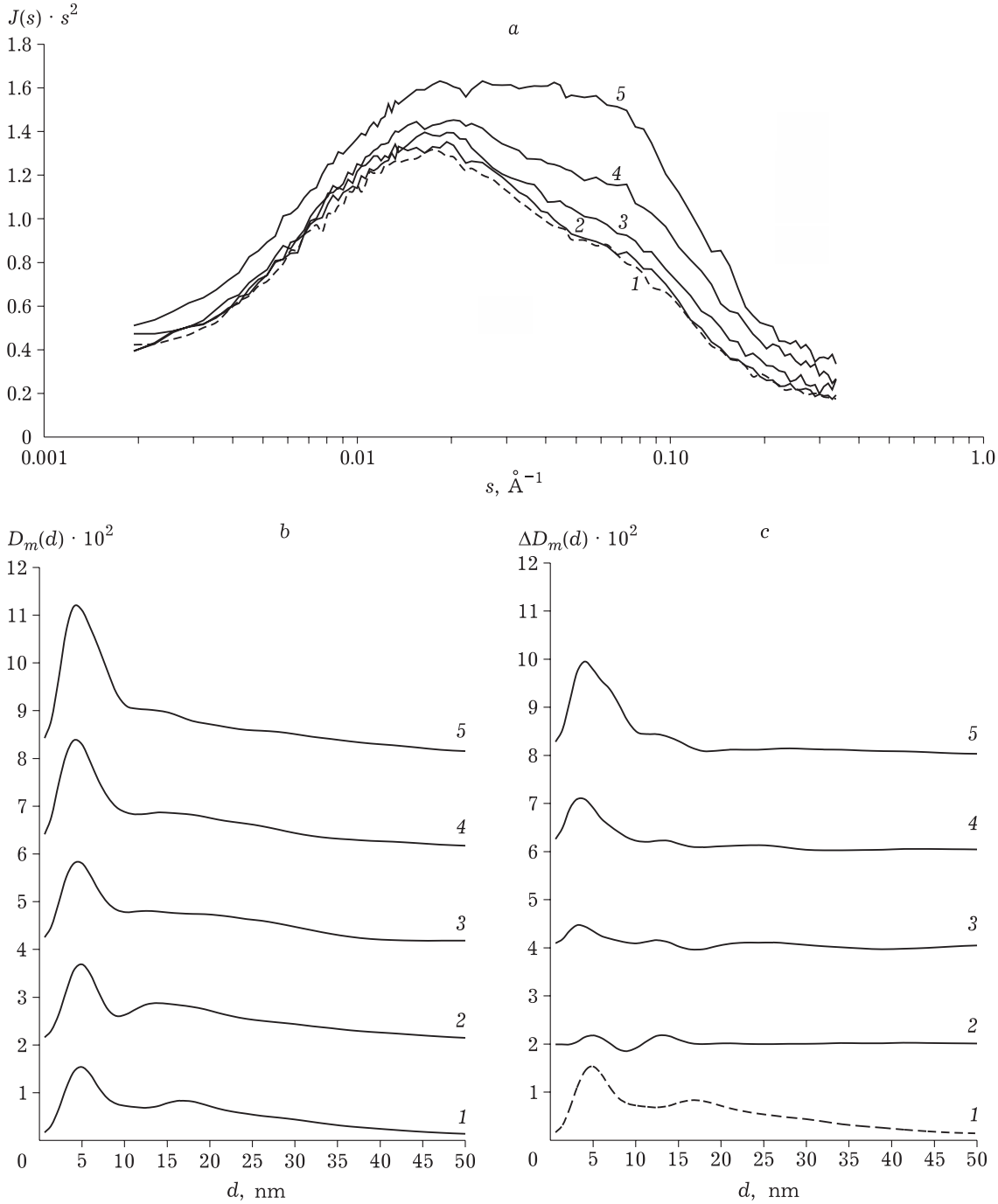

Fig. 3. Experimental curves of small-angle scattering for pure MCNT matrix and for nanocomposite samples (*a*), and calculated functions of the size distribution for nonuniformities (*b* – simple functions, *c* – differential functions) for MCNT matrix and nanocomposite samples $NiCo_2O_4$/MCNT. Metal content in the composite, mass %: 0 (*1*), 1 (*2*), 5 (*3*), 10 (*4*), 20 (*5*).

peated for samples with 5, 10 and 20 %. For the 1 % sample, the differential function $D_m(d)$ is the least reliable one because of the large error in intensity comparable (after subtraction) with the signal itself. Nevertheless, a general similarity with more concentrated samples is evident.

The maximum on the size distribution of nonuniformities in the region of smaller size (4 nm) most probably corresponds to the residual size of cavities inside nanotubes in the sites where they contain the filler from inside. The second maximum (13 nm) is likely due to the arrangement of

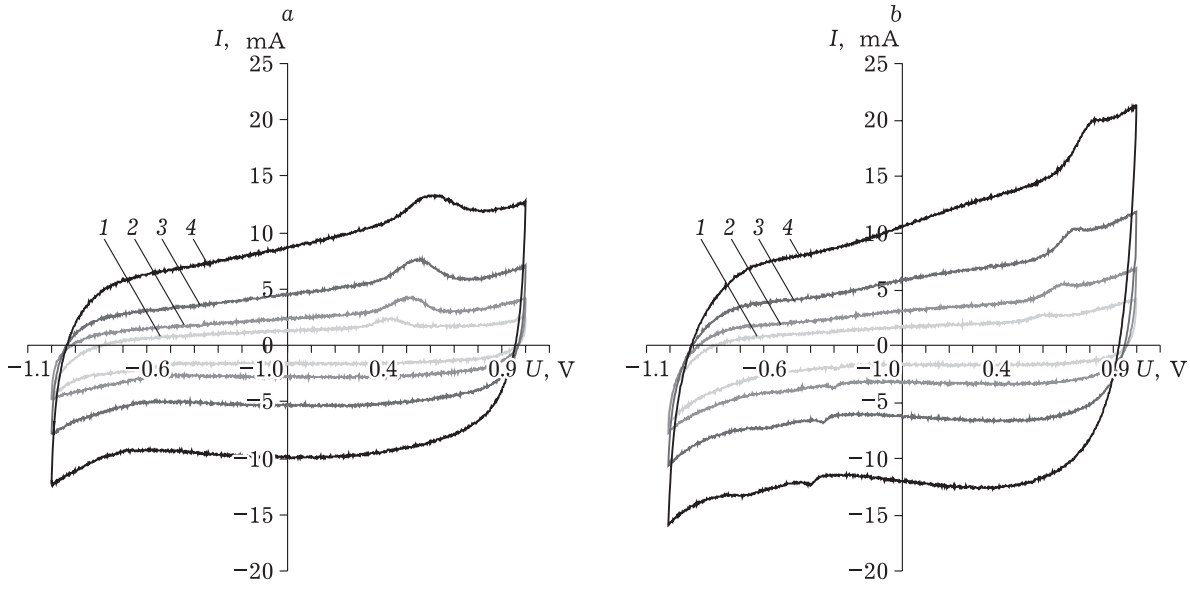

Fig. 4. CVA curves of the asymmetric supercapacitor cell. Working electrode: Co_3O_4/MCNT-10 nanocomposite (*a*) and $NiCo_2O_4$/MCNT-10 nanocomposite (*b*) with counter-electrode made of initial MCNT matrix. Potential scanning rate, mV/s: 10 (*1*), 20 (*2*), 40 (*3*), 80 (*4*).

the filler on the outer surface – in the space between the nanotubes. The large values of $D_m(d)$ function for the first maximum may be due not only to the larger amount of these nonuniformities but also to the higher contrast of the electron density between the empty space and metal-containing filler in comparison with the contrast between this filler and the surrounding carbon material in the second case.

Characteristic features of the correlation functions calculated from the differential SAS signal [7] point to the fact that in the majority of cases the scattering nonuniformities are characterized by two-dimensional morphology. It may be assumed that the particles of the metal-containing phase are formed on the surface of the MCNT matrix in the form of island-like formations 12 to 30 nm thick (for different samples) and not less than 200 nm long.

The appearance of the obtained curves of cyclic voltammetry (CVA) (Fig. 4) points to the presence of a pronounced effect of pseudo-capacity for nanocomposite electrode materials containing $NiCo_2O_4$ and Co_3O_4. For these two types of composites, a similarity of voltammetric curves and the dependences of electrode capacity on the scanning rate is observed (Fig. 5). At the same time, the potentials at which the most intense Faraday processes take place turn out to be different.

The CVA curves of the cells with electrodes made of $NiCo_2O_4$/MCNT-10 nanocomposite (see Fig. 4, *b*) clearly show that within the potential range ±(0.6–0.9) V electrochemical Red-Ox processes participated by the spinel phase of the filler take place in the cathode and anode half-cycles. Due to this component, the capacity of nanocomposite electrodes increases substantially, especially in the case of small potential scanning rates (see Fig. 5, *b*).

A stronger pronounced increase in the capacity of composite electrodes in comparison with MCNT electrodes with a decrease in the scanning rate is connected with a relatively low rate of Red-Ox processes (in comparison with the rate of formation of the double electric layer, DEL, on MCNT electrodes) of the processes participated by the oxide phase, in view of relatively slow diffusion of ions from the electrolyte solution to the electrode surface and in the opposite direction. This agrees with the data of X-ray diffraction patterns on the formation of spinel particles, first, as rather coarse aggregates composed of nanocrystallites, second, not only on the outer surface of MCNT but partially in the channels of nanotubes. In both cases, the access of the electrolyte to the crystallites and in general to the particles of the filler is hindered.

In the case of the electrode material based on Co_3O_4/MCNT-10 composite, the electrode oxidation-reduction processes take place in a narrower potential window and are characterized by lower intensity (see Fig. 4, *a*). This may be due either to the individual features of the electrochemical be-

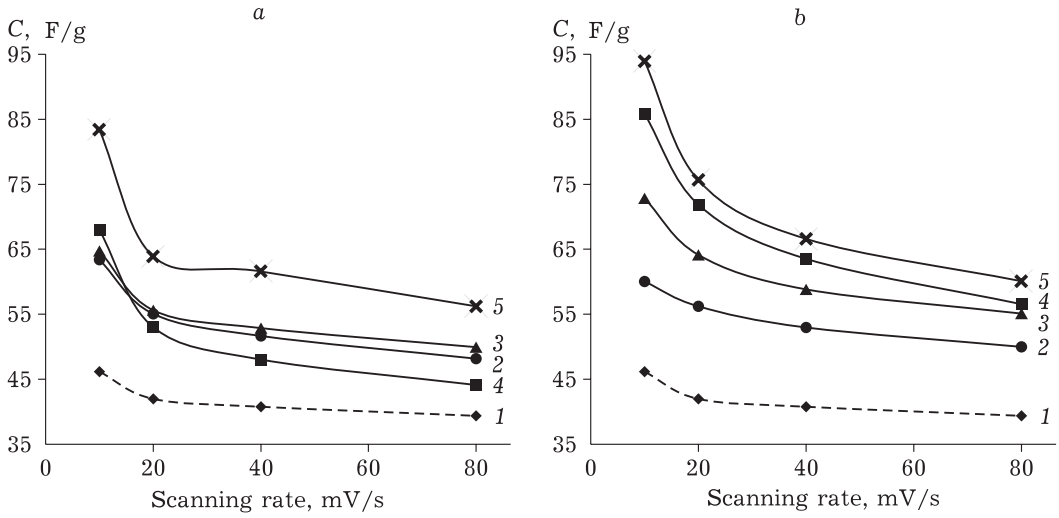

Fig. 5. Dependences of capacity on potential scanning rate for asymmetric cells with working electrodes made of Co_3O_4/MCNT (*a*) and $NiCo_2O_4$/MCNT (*b*) nanocomposites with MCNT matrix as a counter-electrode. Metal content in the composite, mass %: 0 (*1*), 1 (*2*), 5 (*3*), 10 (*4*), 20 (*5*).

haviour of Co_3O_4 or to the difference in the dispersity of products formed in the thermal decomposition of pure cobalt azide and co-precipitated cobalt and nickel azides. This aspect requires further investigation. We also discovered anomalously low capacity (at high scanning rates) of the Co_3O_4/MCNT-10 composite with cobalt content 10 mass %, in comparison with the composites containing 1 and 5 mass %. As the advantages of the electrodes with lower cobalt oxide content manifest themselves only at high scanning rates, it may be assumed that for these composites the carbon surface possessing capacity due to the presence of the double electric layer is blocked by the filler to a lower extent, that is, for materials with the composition Co_3O_4/MCNT the contribution from Faraday processes and from the processes participated by the DEL into total capacity is approximately the same.

CONCLUSION

The possibility to obtain nanocomposite electrode material based on carbon fibres containing mixed oxides of the metals with variable valence through thermal decomposition of the mixtures of metal azides is demonstrated.

The advantages of the mixed cobalt – nickel oxide as the component of the electrode material in comparison with cobalt oxide are demonstrated, from the viewpoint of a total increase in the specific capacity and an increase in the specific capacity at low scanning rates (~10 mV/s).

Acknowledgements

The work was carried out with support from the Integrated Programme of Fundamental Research, SB RAS (Project No. V.46.3.1 0352-2016-0009).

The authors express sincere gratitude to A. S. Chichkan (BIC, SB RAS) for carbon materials of MCNT type submitted for investigation, and to the personnel of the Shared Equipment Centre at the KemSC SB RAS for assistance in experimental studies.

REFERENCES

1 Gonzalez A., Goilolea E., Barrena A., Mysyk R. Review of supercapacitors: technologies and materials, *Renewable and Sustainable Energy Reviews*. 2016. Vol. 58. P. 1189–1206.

2 Yu A., Chabot V., Zhang J. Electrochemical Supercapacitors for Energy Storage and Delivery: Fundamentals and Applications. CRC Press, 2013. 348 p.

3 Lee K. K., Chin W. S., Sow C. H. Cobalt-based compounds and composites as electrode materials for high-performance electrochemical capacitors, *J. Mater. Chem. A*. 2014. Vol. 2. P. 17212–17248.

4 Energetic Materials. Vol. 1. Physics and Chemistry of Inorganic Azides, H. D. Fair, R. F. Walker (Eds.), NY: Plenum Press, 1977. 503 p.

5 Wu Z., Zhu Y., Ji X. $NiCo_2O_4$-based materials for electrochemical supercapacitors, *J. Mater. Chem. A*. 2014. Vol. 2. P. 14759–14772.

6 Li Y., Han X., Yi T., He Y., Li X. Review and prospect of $NiCo_2O_4$-based composite materials for supercapacitor electrodes, *J. Energy Chemistry*. 2018. Vol. 31. P. 54–78.

7 Dodonov V. G., Zakharov Yu. A., Pugachev V. M., Vasiljeva O. V. Determination of the surface structure peculiarities of nanoscale metal particles *via* small-angle X-ray scattering, *Inorg. Materials: Appl. Res.* 2016. Vol. 7, No. 5. P. 804–814.